

ARTICLE

Compact reactor architectures designed with fractals.

Carlos A. Grande,*^a

Received 00th January 20xx,
 Accepted 00th January 20xx

DOI: 10.1039/x0xx00000x

Chemical reactors are the heart of chemical and pharmaceutical plants. Tailored reactors with increased efficiency for specific applications can move industry a step forward towards a better environmental performance. Advances in manufacturing techniques expanded the possibilities to produce customized reactors. This work presents a novel methodology to design reactors based on fractal mathematics in a software that is not commonly used in chemistry or chemical engineering. The designed geometry was used to predict the residence time distribution as an indicator of the reactor performance. This new approach offers the possibility to manufacture compact, efficient and customizable 2D and 3D reactors that can be coupled with ancillary equipment to enhance mass and heat transfer.

Introduction

Transformation of reactants into valuable products take place in reactors. By transforming reactants into products, chemical and pharmaceutical industries have transformed the quality of our everyday life. Safe and widely available products have significantly contributed to modernize our lifestyle. The next challenge in those industries is to improve the environmental performance by decreasing energy consumption and reducing waste. Under certain conditions, increase in efficiency will directly lead to reduced production costs.

In recent years, switching from batch to continuous reactors was recognized in many fields as a step forward in performance, energy and resource utilization, safety, etc.¹⁻⁸ Common terms for this paradigm shift are continuous manufacturing and flow chemistry, while a more generic term "continuous reactors" is traditionally used in chemical engineering. There has been significant amount of work to intensify the operation of reactors, particularly regarding continuous manufacturing of APIs (active pharmaceutical ingredients) or flow chemistry in production of fine chemicals.⁹⁻¹⁰

Due to economics of reactor manufacturing, many reactor configurations assume the shape of cylindrical vessels (i.e. tubular reactors) and the scale-up of such reactors is done by increasing the tube diameter. There have been alerts that under some circumstances, heat transfer effects may result in lack of performance.¹¹ A traditional solution for those cases is to apply bundles of tubes in multi-tubular reactors increasing the area for heat transfer. Heat-transfer related issues increase significantly for very strong exothermic or endothermic reactions. In such systems, either complex reactor configurations or feed dilutions are used. The ultimate objective is to design a reactor that can deal with heat transfer and can be scaled in an economically viable manner.

The utilization of 3D printing enables exploration of different geometries for reactor design in ways that no other manufacture technology has allowed before.¹² The optimization of the reactor can be done before manufacturing the first demonstrator, combining parametric design and advanced modelling. Nowadays the cost of 3D printing a reactor in metal is rather high, but with a decreasing trend. Costs can decrease further after industrial applications are deployed. However, even with the current costs, production of expensive fine chemicals and APIs is possible; the increased cost in the reactor can be balanced by increased performance.

Fractals are interesting mathematical functions and the possibility to use them as shape generators for a fluid pathway provides a new methodology to design reactors that resemble nature. Fractals are infinitely complex patterns that are self-similar across different scales. They are created by repeating a simple process over and over in an ongoing feedback loop.¹³ The term fractal comes from the Latin fractus meaning broken or fractured. Nature has multiple examples of fractals, although it has been argued that the attribution of fractals to shapes in nature is merely an approximation.¹⁴ The use of fractals is in line with a very interesting approach followed by Prof. Coppens based on the concept of Nature-Inspired Chemical Engineering (NICE).¹⁵

Fractal mathematics were already used to create diverse unitary operations in chemical engineering. There are examples of mixers, gas distributors and different types of reactors for several applications.¹⁶⁻²³ Those publications serve as inspiration to develop the generic methodology presented in this work that can easily describe 2D and 3D fractals indistinctively. While developing the methodology, it was noted that there were not continuous flow reactors produced with a unique 3D fractal curve and as will be shown in this work, such approach can provide additional advantages not yet analysed in literature.²⁴ In this publication, the methodology used for the design, modelling and manufacturing of fractal reactors is given. Although the reactors can be manufactured by 3D printing, other techniques can be used, particularly for the 2D designs. A

^a SINTEF AS, Forskningsveien 1, 0373, Oslo, Norway.
 Electronic Supplementary Information (ESI) available. See DOI: 10.1039/x0xx00000x

series of common fractals were used for 2D and 3D reactor design and then used to model the residence time distribution (RTD). Note that the main aim of this publication is to present a flexible design methodology that can be applied in multiple applications. For this reason, the manufacturing of some demonstrators of these reactors are shown as Supporting Information.

Digital methodology

One special case of fractals are the so-called "space-filling curves".²⁵ A space filling curve provides a continuous map of a one-dimensional interval into a two-dimensional area or of a three-dimensional volume. Any space-filling curve should pass only once through every cell element of the defined space (2D or 3D). A X-dimensional space-filling curve in a domain of N cells of each dimension consists of $NX - 1$ segments where each segment connects two consecutive points.

The first reported space-filling family of curves is the Peano curve. The Peano curve can pass through every point of the unit square.²⁶ Other fractals, like the Hilbert or Moore families of space-filling curves, were discovered slightly later. The Hilbert and Moore curves (as well as many other 2D space-filling curves) can be expanded to three dimensions.

One simple way to describe space-filling curves is the Lindenmayer system, typically called L-system.²⁷ The L-system is composed by an "axiom" (normally described by a letter of the alphabet) and one or more "reproduction rules" that are repeated a certain number of times and result in a string. In the reproduction rules, it is possible to introduce commands that will help the string to be interpreted by a separate mechanism and adapt it to a geometrical shape. The number of times that a set of reproduction rules is repeated correspond to the iteration or the "pseudo-order" of the fractal. The L-system instructions are simple and normally associated to the historical term "turtle motion". Instructions like "+" means turn left, "-" means turn right, while "&" indicates a pitch down, etc. A certain angle should be defined for those operations; while 90° is used in many curves, other values are used in other space filling curves. The sequence of the 2D Hilbert curve can be produced by defining an axiom L with the following production rules:

$$L = +RF - LFL - FR + \quad (1)$$

$$R = -LF + RFR + FL - \quad (2)$$

An angle of 90° should be used for the Hilbert and Moore curves. The 3D Hilbert curve syntax is more complex, once that the movement should be described in three dimensions. The curve has an axiom A and production rules given by:

$$A = B - F + CFC + F - D&F^A D - F + \&\&CFC + F + B / / \quad (3)$$

$$B = A&F^A CFB^A F^A D^A - F - D^A |F^A B|FC^A F^A A / / \quad (4)$$

$$C = |D^A |F^A B - F + C^A F^A A&F^A F^A C + F + B^A F^A D / / \quad (5)$$

$$D = |CFB - F + B|FA&F^A A&\&FB - F + B|FC / / \quad (6)$$

Also, an angle of 90° should be used. There are different software able to generate these families of fractals. In this work, Rhinoceros 6 (McNeel & Assoc., USA) has been used for that purpose. To make the system parametric, the entire code was implemented in Grasshopper, the parametric environment within Rhinoceros. While this software is not used yet in chemical and chemical engineering applications, it is extremely flexible for advanced geometrical design and it also produces high-quality meshes that can be directly exported to more traditional software used for computational fluid dynamics (CFD). There are different methods to generate fractals in Grasshopper. The Rabbit plugin offers a simple methodology to generate the fractal curves via L-system coding and turtle motion interpretation.²⁸ The code to generate and evaluate the properties of the 2D Moore curve is shown in Figure 1.

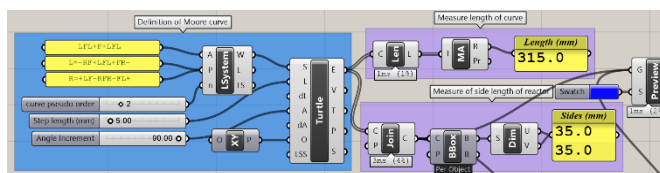


Fig. 1. Generation of Hilbert curve within Grasshopper using the L-system notation and turtle motion graphics.

The L-system notation of other common 2D fractals that were produced using this methodology is given in Table S1. The fractals provided in Table S1 constitute a non-exhaustive list and they are only given to demonstrate vast possibilities of tailoring the reactor design.

The specific functionalities presented can be tuned to adapt the reactor for a particular application. The overall reactor length can be controlled by the length of each step and by changing the pseudo-order. Moreover, the axiom can be modified to change the location of the inlet-outlet connection ports. One important property of all the space-filling curves (shown in Figure 1), is that a long tube can be efficiently folded into a very small reactor volume. In Table 1, the dimensions of a reactor using different pseudo-orders or iterations of the Moore or Hilbert curves are shown (using a step length of 5 mm).

Table 1. Length and reactor area of different pseudo-orders of a 2D Moore (and Hilbert) curves with step length of 5 mm.

Pseudo order	Curve length [mm]	Reactor area [mm ²]
1	15	25
2	75	225
3	315	1225
4	1275	5625
5	5115	24025
6	20475	99225
7	81915	403225

The results from Table 1 indicate that with this configuration it is possible to have a reactor length of ~ 82 meters in a parallelepipedal reactor with a larger side length of ~ 0.4 m.

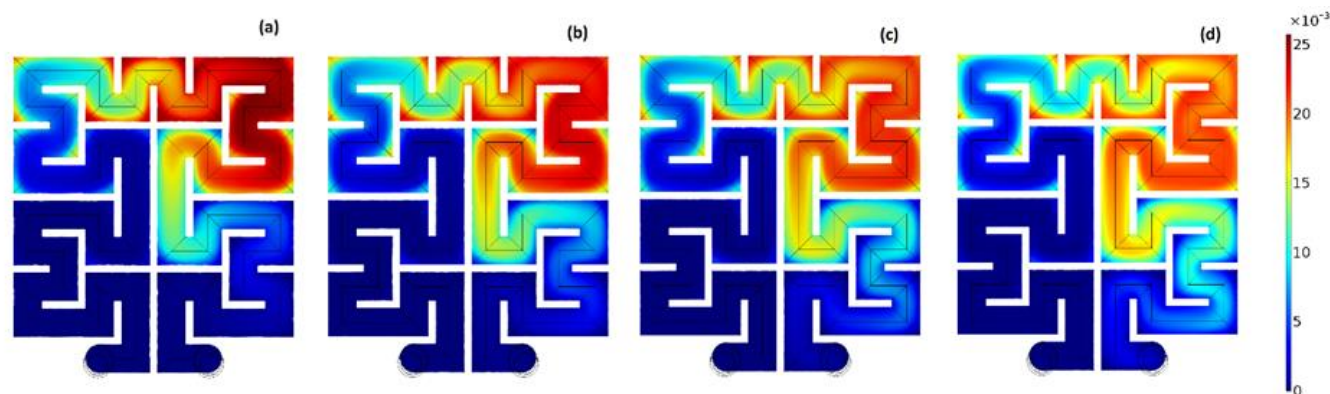


Fig. 2. Plot of concentration at 50 seconds after injection of a pulse of tracer using a velocity of 0.01 m/s for meshes with different number of elements: (a) 81448, (b) 288047, (c) 942975 and (d) 1793241 elements.

When the 3D Hilbert or Moore curves are used, the values obtained should be given in terms of reactor volume once the curve is three dimensional. The tube is arranged in a 3D volume instead of a flat surface, so it is possible to obtain much larger reactor length within a smaller plot area. As shown in Table S2, with the 3D Hilbert or 3D Moore curves, it is possible to achieve a reactor length of ~ 163 m with a cubic reactor with side length of ~ 0.16 m. The reactor length obtained with the 3D Hilbert or Moore curves is the same as what can be obtained by replicating the 2D Hilbert or Moore curves in the same volume.

CFD results

One of the main benefits of producing chemical reactors using digital technologies like 3D printing is that the performance of the reactor can be evaluated before its manufacture. For this initial presentation of the design methodology, the residence time distribution (RTD) function was chosen since it provides very valuable information of the reactor that has been designed.²⁹⁻³² However, the customization of reactors for a given application requires detailed knowledge about the reaction kinetics, the flow regime and in some cases, details on the heat transfer. The RTD can be obtained by running CFD simulations over the internal shape of the reactor from a CAD (computer aided design) file, which is the starting point of the process. Running simulations in turbulent regime may require surface topology parameters that are specific to the manufacture method. Since the objective of this work is to present a generic design, only results in laminar flow regime will be provided.

The first thing to be noted from Figure 1 is that the inlet / outlet of the reactor may need some changes to connect the reactor to an external system, which can be done by slightly changing the axiom. For the case of the Moore curve represented in Figure 1, a simple change in the axiom to $FF^{\wedge}FLFL+F+LFLF^{\wedge}FF$ can solve the connectivity issues. The produced shape has to be "baked" (name of command in Grasshopper to place the geometry in the Rhinoceros domain). The geometry can be exported in a variety of formats. An *.stl file can be exported to a CFD software, like COMSOL Multiphysics. The geometry and its mesh are shown in Figure S1 as an example. The stl file of the

initial reactor designed with the shape given in Figure 1 (reactor 1) is also provided as Supporting Information.

Using Navier Stokes coupled with a mass balance in transient mode is possible to obtain the residence time distribution of the reactor. For the RTD simulations, a Gaussian pulse was used as input for the tracer component. Only the standard options of physics from COMSOL Multiphysics were used in this work: transport of diluted species and Laminar flow. To integrate the concentration over the area of the tube at the outlet of the reactor, a "probe" option (also default in COMSOL) was used. Despite all the default and simpler options were used, it is important to have a mesh with a good quality to get representative results. Different meshes were used with increasing quality. For the initial reactor (2D Hilbert or Moore), the simulations were made using 81448, 288047, 942975 and 1793241 elements to evaluate the needed mesh quality to obtain reproducible results. For this geometry, almost 2 million elements were necessary to obtain good results. The reason for that is the difficulty to remove the tracer from the corners of the channels as shown in Figure 2. When a low number of elements is used, the edges are incorrectly described with a smaller number of elements. The concentration at the exit of the reactor as a function of time for the different meshes is given in Figure S2 in the Supporting information.

The difficulty in removing the tracer compound from the edges of the reactor leads to a larger concentration tail in the RTD curve, which is not desired for many applications. The tail can be mitigated by reducing the sharp edges and can be achieved by for example by rounding the corners. Using these fractals, just a simple corner rounding did not provide a significant advantage, so the channel tubes were slightly bended. While at the lower inlet velocities (0.01 m/s) small changes are noted, for the simulations with a higher inlet velocity (0.05 m/s), there is a significant reduction in the concentration tail exiting the reactor. The bending of each segment of the fractal leads to a reduction in the total length of the reactor and depends on the extent of the rounding. For an internal tube radius of 2 mm, a rounding of 2 mm leads to a length reduction of 14% (leading to 14% volume reduction). To further reduce the tail of the concentration curve it is also important to smooth all possible variations in diameter of the reactor and the connectors. The

effect of the different parameter variations to the initial design are shown in the Supporting Information.

3D fractals & architectural flexibility

Extending the concept of the fractal reactors is possible once that there are several fractal space filling curves already developed for this purpose. The second iteration of the Moore curve in 3D has a similar length as the third iteration of the 2D Moore curve. However, the 3D reactor has 1/4 of the area of the 2D Moore (is therefore larger in the z-direction). This plot area reduction is important for several 3D printing technologies that are associated to a "printable area". Attention must be given to the type of connector ports that are expected; the Moore curve by default has the inlet / outlet tubes very close and the use of external connection ports may be problematic if the tubes are not separated (as done in the 2D case).

The results on the 2D reactor are shown in Figure 3 while the ones for the 3D reactors are shown in Figure 4. It should be mentioned that the volume of the 2D and the 3D Moore reactors is not the same. The tube bending in 3D has resulted in a slightly shorter reactor (less than 5% difference in volume). This is caused by the tube bending in two and three dimensions. Nevertheless, this small difference in volume does not justify the better performance of the 3D version as observed in the

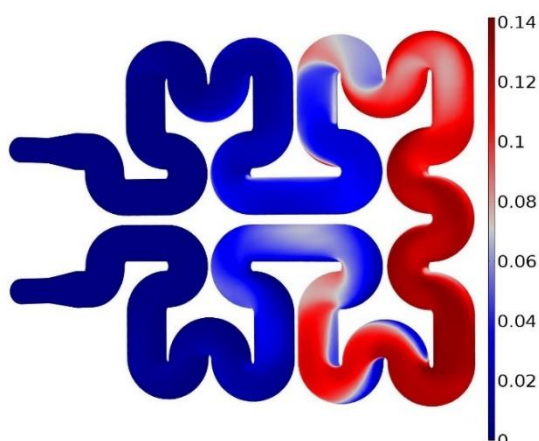
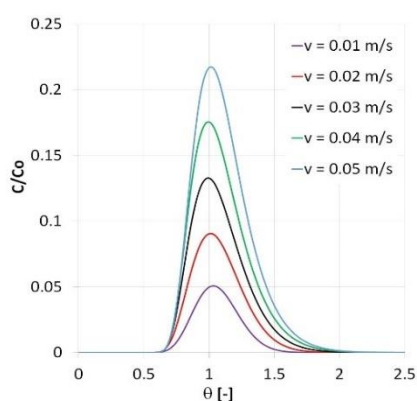


Fig. 3. RTD functions at different velocities for a reactor made with a third iteration of the 2D Moore and concentration distribution at $t = 8$ seconds (for $v = 0.05$ m/s).

RTD. The 3D bending of the tubes of the reactor does contribute to generate a more homogeneous vorticity which improves the mixing.³³

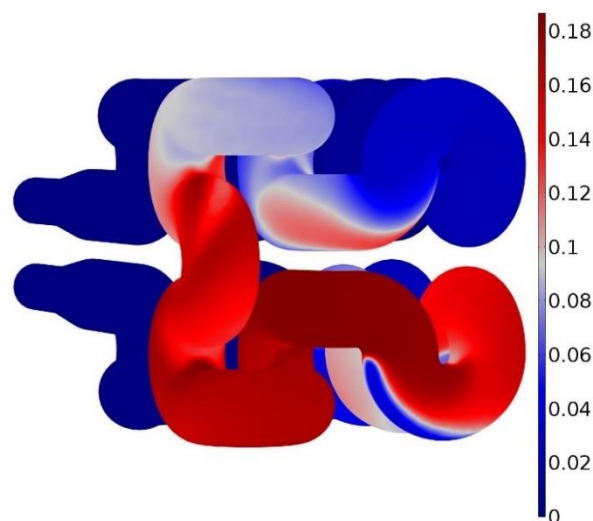
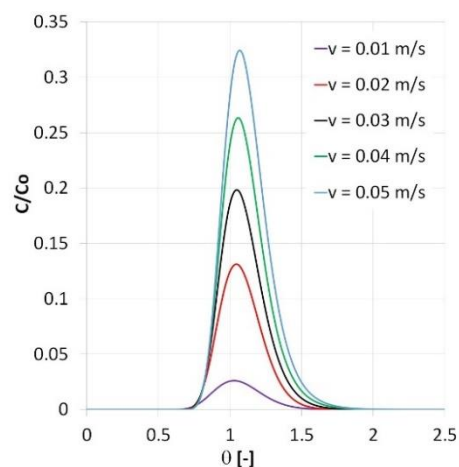


Fig. 4. RTD functions at different velocities for a reactor made with a second iteration of the 3D Moore and concentration distribution at $t = 8$ seconds (for $v = 0.05$ m/s).

An important design advantage of the fractal 3D reactors is their compactness. Very long reactors can be obtained by a proper "folding" of the tubing. Using space-filling curves, the tube folding is extremely ordered and it is possible to produce a long reactor with much less material than a normal tubular reactor, particularly for operating at higher pressures. For such cases, the reactor can have a rather thin layer between the internal tubing and only a thicker layer on the outside. This can contribute to significant savings in the construction of the reactor.

Whether in 2D or 3D, the different families of space-filling curves provide an enormous flexibility for reactor design. The length can be tailored, the degree of mixing can be adjusted by changing to curves with different number of bending segments or different angles, or the reactor can be integrated with other elements to enhance the degree of mixing or mass and heat transfer.

Additionally, changes to the channel architecture can be performed. Instead of the traditional pipes, other shapes (with at least three sides) can be used. These shapes will change the volume of the reactor and the surface area to volume ratio, which has an important impact in heat transfer. Moreover, the surface area can be increased by twisting the channels in a certain degree, with impact on the heat and mass transfer. Examples of the reactors mentioned here are shown in the Supplementary Information.

Concatenated fractals can also be used to overcome the traditional cubic design of standard fractals, making it possible to change the initial cubic shape to a parallelepipedal shape. Alternatively, the design of these fractal curves can be adapted to any geometry that may render better performance of the reactor. For example, the reactor can be produced with a curvature to increase sun light exposure.

The main message of this communication is that the alliance between mathematical functions and manufacturing techniques can render reactor designs that were not possible just few years ago. While this work presents the work done using fractals, it is possible to design other reactors purely based on mathematical functions. If this is done parametrically, the modelling of a scaled-up reactor and its manufacturing should be faster, as well as the utilization of similar designs for other applications.

Conclusions

In this publication, a new and generic methodology to design reactors based on fractals is presented. Reactors using a 2D as well as 3D fractal structures can be designed, evaluated before manufacturing, and produced by 3D printing. Although the methodology was idealized for reactor manufacturing by 3D printing, there are other advanced manufacturing techniques that can be used for producing them, particularly the 2D versions. The 3D family of fractal reactors offer enormous possibility of tailoring, from the basic architecture concatenating fractals or adapting to other external shape constraints to specific changes in the channel geometry and rotation. The important advantage of this methodology is the possibility of producing tailored reactors that can be adapted to multiple applications for continuous manufacturing in chemical and pharmaceutical industries.

Conflicts of interest

The fractal reactors shown in this publication are some of the examples used to fill a patent application; reference 19 cited in this work.

Acknowledgements

Special acknowledgment to T. Yorke, J. Greenwood, C. Greenwood, E. O'Brien and P. Selway for the inspirational nature of their work.

References

- 1- V. Hessel, *Chem. Eng. Technol.*, 2009, **32**, 1655–1681.
- 2- L. X. Yu, *Pharm. Res.*, 2008, **25**, 781–791.
- 3- R. L. Hartman, J. P. McMullen and K.F. Jensen, *Angew. Chem., Int. Ed.*, 2011, **50**, 7502–7519.
- 4- P. Plouffe, A. Macchi and D.M. Roberge, *Org. Process Res. Dev.*, 2014, **18**, 11, 1286–1294.
- 5- J.G. Costandy, T.F. Edgar and M. Baldea, *Ind. Eng. Chem. Res.*, 2019, **58**, 30, 13718–13736.
- 6- J.R. Burns and C. Ramshaw, *Chem. Eng. Res. Des.*, 1999, **77**(3), 206–211.
- 7- D.M. Roberge, M. Gottsponer, M. Eyholzer and N. Kockmann, *Chem. Today*, 2009, **27**(4), 8–11.
- 8- J. Zhang, K. Wang, A.W. Teixeira, K.F. Jensen and G. Luo, *Annu. Rev. Chem. Biomol. Eng.*, 2017, **8**(13), 1–13.21.
- 9- A. Roibu, C.R. Horn, T. Van Gerven and S. Kuhn, *ChemPhotoChem*, 2020, **4**(10), 5193–5200.
- 10- A. Steiner, P.M.C. Roth, F.J. Strauss, G. Gauron, G. Tekautz, M. Winter, J.D. Williams and C. O. Kappe, *Org. Process Res. Dev.*, 2020, **24**, 10, 2208–2216.
- 11- N. Yazdanpanah, C.N. Cruz and T.F. O'Connor, *Comp. Chem. Eng.*, 2019, **129**, 106510.
- 12- C. Parra-Cabrera, C. Achille, S. Kuhn and R. Ameloot, *Chem. Soc. Rev.*, 2018, **47**, 209–230.
- 13- B.B. Mandelbrot, *The fractal geometry of nature*. W.H. Freeman, San Francisco, USA, 1982.
- 14- O.R. Schenker, Fractal geometry is not the geometry of nature. *Studies Hist. Phil. Sci. A*, 1994, **25**, 967–981.
- 15- M.-O. Coppens, *Curr. Op. Chem. Engng.*, 2012, **1**, 1–9.
- 16- P. Trogadas, V. Ramani, P. Strasser, T.F. Fuller and M.-O. Coppens, *Angew. Chem., Int. Ed.*, 2016, **55**, 122–148.
- 17- B. Ramos-Alvarado, A. Hernandez-Guerrero, F. Elizalde-Blancas and M.W. Ellis, *Int. J. Hydrogen Energy*, 2011, **36**, 12965–12976
- 18- P. Trogadas, J.I.S. Cho, T.P. Neville, J. Marquis, B. Wu, D.J.L. Brett, and M.-O. Coppens, *Energy Environ. Sci.*, 2018, **11**, 136–143.
- 19- Y. Lu, G. Wang, Z. Liang, J. Sun, Y. Gu and Z. Tang. *Int. J. React. Engng.*, 2018, 20170225.
- 20- S. Zhang, Y. Lu, Y. Gu, X. Zhang, J. Sun and Z. Tang. *Chem. Eng. Proc. Proc. Intensif.*, 2018, **132**, 42–47.
- 21- L. Zhao, G. Zeng, Y. Gu, Z. Tang, G. Wang, T. Tang, Y. Shan and Y. Sun. *Chem. Eng. Sci.*, 2019, **193**, 6–14.
- 22- G. Wang, Y. Gu, L. Zhao, J. Xuan, G. Zeng, Z. Tang and Y. Sun. *Chem. Eng. Sci.*, 2019, **195**, 250–261.
- 23- J. Zhang, S. Zhang, C. Peng, Y. Chen, Z. Tang and Q. Wu. *React. Chem. Eng.* 2020, **5**, 2250–2259.
- 24- C.A. Grande, *Fractal reactors*. U.K. Patent application 2014930.8, 2020.
- 25- M. Mokbel and W. Aref, *Space-Filling Curves*. In: Shekhar S., Xiong H. (eds) *Encyclopedia of GIS*. Springer, Boston, MA, 2008.
- 26- P. Prusinkiewicz and A. Lindenmayer, *The algorithmic beauty of plants*. Springer-Verlag, New York, 1990.
- 27- A. Lindenmayer, *J. Theoret. Biol.*, 1968, **18**, 300–315.
- 28- Rabbit. Plugin for Grasshopper. Available at: <https://morphocode.com/rabbit/>.
- 29- A.E. Rodrigues, *Chem. Eng. Sci.*, 2021, **230**, 116188.
- 30- P. Toson, P. Doshi and D. Jajcevic, *Processes*, 2019, **7**, 615.
- 31- Y. Gao, F.J. Muzzio and M.G. Ierapetritou, *Powder Technol.*, 2012, **228**, 416–423.
- 32- V. Sans, N. Karbass, M.I. Burguete, E. García-Verdugo and S.V. Luis, *RSC Advances*, 2012, **2**, 8721–8728.
- 33- I.A. Waitz, Y.J. Qui, T.A. Manning, A.K.S. Fung, J.K. Elliot, J.M. Kerwin, J.K. Krasnodebski, M.N. O'Sullivan, D.E. Tew, E.M. Greitzer, F.E. Marble, C.S. Tan and T.G. Tillman, *Prog. Aerospace Sci.*, 1997, **33**, 323–351.